Powder Technology 431 (2024) 119057

Contents lists available at ScienceDirect

Powder Technology

journal homepage: www.journals.elsevier.com/powder-technology

Short Communication

Transient jamming of granular flow by blade spreading

Wenguang Nan [a,b,*], Lanzhou Ge [a], Wenbin Xuan [a], Yiqing Gu [a,c]

[a] School of Mechanical and Power Engineering, Nanjing Tech University, Nanjing 211816, China
[b] Faculty of Engineering and Physical Sciences, University of Leeds, Leeds LS2 9JT, UK
[c] School of Mechanical and Power Engineering, East China University of Science and Technology, Shanghai 200237, China

HIGHLIGHTS

- Jamming forms and collapses under the effects of narrow gap and blade shearing.
- Angular particles with weak cohesion are more prone to mechanical jamming.
- Cohesion-induced jamming is critical for the empty patches within spread layer.
- A regime map is experimentally deduced for the transient jamming by spreading.

GRAPHICAL ABSTRACT

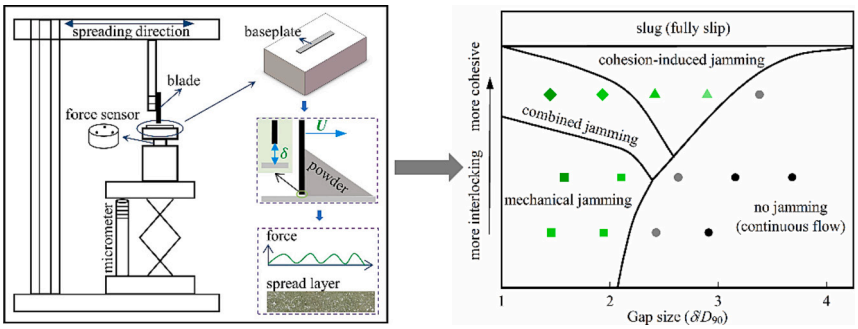

ARTICLE INFO

Keywords:
Spreading
Particle flow
Jamming
Rheology

ABSTRACT

This work focuses on a new kind of jamming of particle flow through constriction, which occurs in the powder spreading process in additive manufacturing, i.e. a powder heap is spread onto a rough surface by a moving blade. This work shows the experimental evidence of transient jamming by blade spreading at the first time. The jamming repetitively forms and collapses under the combined effects of narrow gap and blade shearing action. Angular particles with weak cohesion are more prone to mechanical jamming, with longer survival time of jammed state and stronger jamming strength. Besides mechanical jamming, cohesion-induced jamming is also responsible for the formation of empty patches within the spread layer. A regime map is deduced from physical experiments for the transient jamming by blade spreading in additive manufacturing, depending on the gap size, particle shape, and particle cohesion.

1. Introduction

Reliable control of powder flow through constrictions is of great interest in particle processing industries. A major recent example is powder spreading technology in additive manufacturing, i.e. a powder heap is spread onto a rough baseplate by a blade or roller spreader to form a thin layer [1], where the gap between the spreader and the baseplate surface is only a few multiples of particle diameter. In this case, the prediction and control of the rheological behaviour [2–5] of particles and the quality of the spread layer for subsequent manufacturing [6] are significantly affected by the transient jamming, as initially reported by the numerical work of Nan et al. [7] using

* Corresponding author at: School of Mechanical and Power Engineering, Nanjing Tech University, Nanjing 211816, China.
E-mail address: nanwg@njtech.edu.cn (W. Nan).

https://doi.org/10.1016/j.powtec.2023.119057
Received 13 July 2023; Received in revised form 3 October 2023; Accepted 12 October 2023
Available online 15 October 2023

Discrete Element Method. The jamming of particles through constrictions has been extensively studied in several particulate systems, such as hopper flow driven by gravity [8,9], belt flow driven by friction [10,11], pipe flow driven by fluid [12,13], where the jamming is usually in a static equilibrium with particle flow permanently halted. Meanwhile, some work has also been carried out on the jamming in the shearing system of bulk particles, such as simple shear cell or 2D Couette shear cell [14–16], but the constriction is not involved as the gap between moving and stationary walls is constant everywhere. Till now, little work has been made on the physics of jamming during powder spreading in additive manufacturing, in which the particulate system is comprised of a stationary wall supporting a particle heap and a moving blade spreading the heap horizontally. In this work, through experimental investigation, we show in the first instance that the jamming by blade spreading is much different to the ones explored in previous work. By analysing the force on the baseplate and the image of the spread layer in the experiment, the physics of transient jamming is analysed, following which a regime map of induced jamming is defined. The results will have a notable impact on the further understanding of the nature of jamming in particulate system, and the technology of powder spreading in additive manufacturing.

2. Method

The experimental system mainly consists of a spreading blade, a baseplate with a force sensor underneath it, as shown in Fig. 1. The size of the gap between the blade tip and baseplate surface is precisely controlled by a lifting platform with a micrometre calliper, and calibrated by a series of feeler gauges with minimum thickness of 10 μm, in which the feeler gauge is inserted into the gap to make sure the gap size is at the set value. The gap size δ is re-examined by the feeler gauge after spreading. The powder is fed into the front of the blade by a micro-vibration feeder, then the force sensor is re-set to zero, and the powder heap begins to be spread onto the baseplate by the blade with a thickness of 1 mm. The blade moves at a constant velocity U (i.e. 0.01 m/s), which is controlled by a linear servo motor (ASD-A2, Delta Electronics Inc., Taiwan, China) with high accuracy. Before each experimental test, the baseplate is carefully cleaned by a brush and vacuum cleaner, to make sure there are not any particles residual on the baseplate, and the gap size is adjusted again and examined, even if two successive tests are at the same spreading condition. The powder is used only once and discarded after each experimental test.

To address the effects of particle cohesion and particle shape on the particle jamming, three kinds of powder are used: 1) powder A: 316L stainless steel powder made by plasma-rotating electrode, the particle shape of which is almost spherical, and the cohesion is weak; 2) powder B: sand powder, the particle shape of which is angular, and the cohesion is weak; 3) powder C: sand powder coated by a binder. Compared to powder B, particle shape in powder C is almost similar but the cohesion between particles is much stronger. All of them are used in the industry of additive manufacturing, i.e. Powder A in Electron Beam Melting (EBM) of metal parts, while Powder B and powder C in binder-jet printing of sand moulds. The volume-based and number-based D_{10}, D_{50} and D_{90} as well as SEM images of particles are shown in Table 1 and Fig. 2, respectively. If not specified, number-based D_{90} is used as the characteristic particle diameter. For powder A ($D_{90} = 103$ μm), the gap size of 150, 200, 250, and 300 μm is used. For powder B ($D_{90} = 190$ μm) and powder C ($D_{90} = 207$ μm), the gap size of 300, 400, 500, 600, and 700 μm is used. For the baseplate, the length (i.e. in the spreading

Table 1
Physical properties of particles used in the experiment.

Powder	Material	Volume-based D_{10}, D_{50}, D_{90} (μm)	Number-based D_{10}, D_{50}, D_{90} (μm)	Repose angle (°)
A	316L stainless steel	62, 91, 130	48, 70, 103	25
B	Sand powder	111, 173, 268	87, 123, 190	38
C	Sand powder with binder	125, 185, 272	100, 140, 207	51

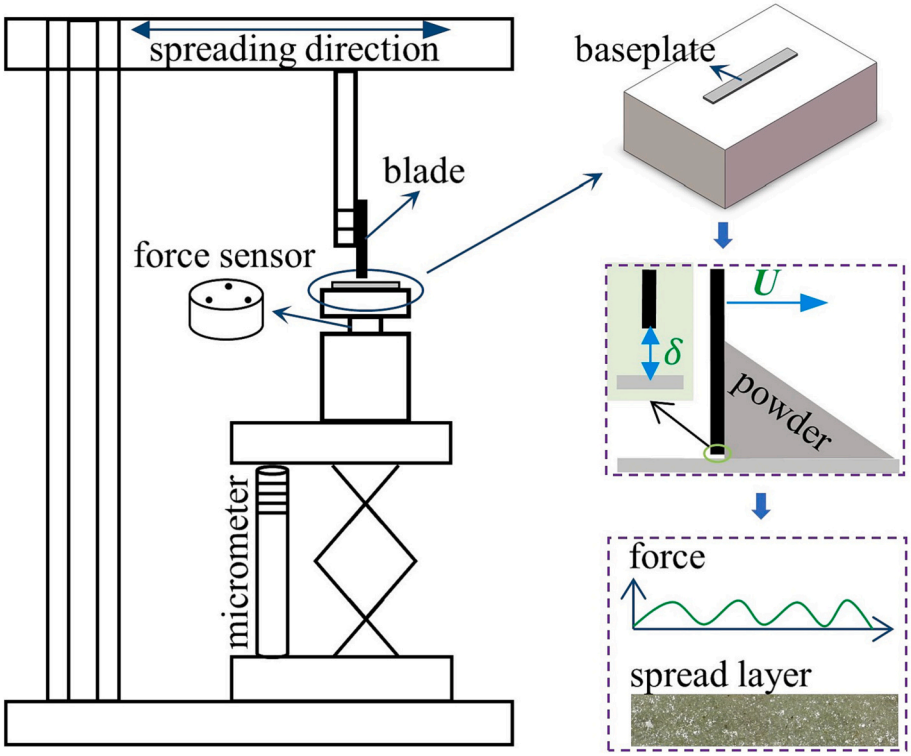

Fig. 1. Diagram of blade spreading system of particles, where the gap between the blade tip and baseplate surface is only a few multiples of particle diameter D_{90}.

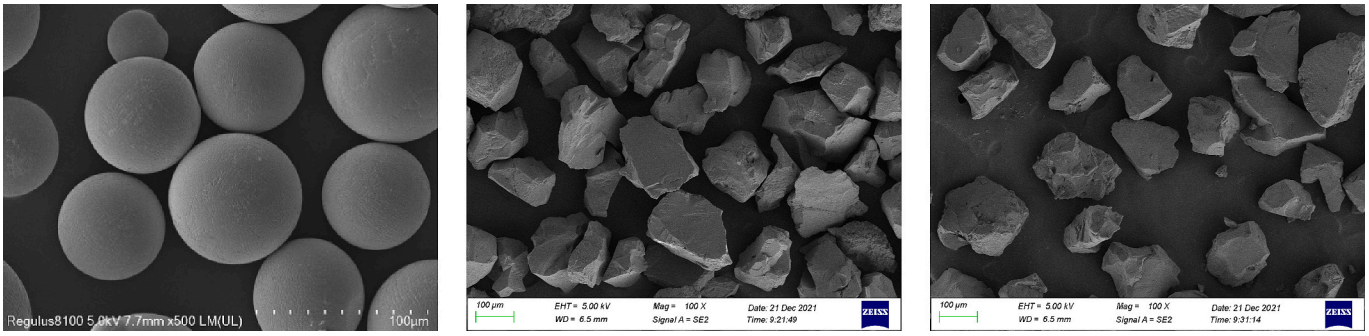

Fig. 2. SEM image of particles used in experiments: powder A (left), powder B (middle), and powder C (right).

direction) is 25 mm, and the widths are 3 mm for powder A, and 5 mm for both powder B and powder C, respectively. For each spreading condition, 11 experiments are carried out, to make sure that the averaged results not further affected by more repetitive experiments anymore. The experiment is carried out in normal atmospheric environment. Due to large particles and low spreading speed used in this work, the effect of fluid medium or interstitial gas on the spreading system could be ignored [17,18]. The force on the baseplate is measured by a force sensor (SBT674, Simbatouch Inc., Shenzhen, China) during the spreading process, and the image of the spread layer is obtained by an optical camera after spreading.

3. Results and discussions

Fig. 3(a) shows the experimental evidence of mechanical jamming in the blade spreading system. There are several force peaks when the gap is narrow, which is caused by the strong force chain during the survival period of jamming. In the case of $\delta/D_{90} = 1.58$, the force could even jump to 1 N when jamming is occurred. However, the force chain is not stable, and it would be quickly broken under the shear action of the moving blade, but later it could occur again. Therefore, the jamming in blade spreading system is transient and in a dynamic state, i.e. repetitively forming and collapsing. A schematic of two kinds of possible states of the jammed particles in the mechanical jamming is suggested in Fig. 3 (b), where the force chain could only resist the load from blade action in the spreading direction. This new kind of jamming is much different to the jamming [8,14] in hoppers, where the particle flow is permanently stopped after the occurrence of jamming, and the jammed particles are in a static equilibrium. It is also different to the intermittent jamming described by stress-strain relation in the quasistatic shearing system of bulk frictionless particles, as simulated by Heussinger [19], where the jamming is mainly determined by the critical particle volume fraction. As the gap size δ/D_{90} increases from 1.58 to 2.11, both the maximum force and the number of force peaks are significantly reduced. At the gap size of $\delta/D_{90} = 2.63$, almost no mechanical jamming could be observed. For powder A and powder C, a similar trend is observed, as shown in Appendix.

Continuous data points in Fig. 3(a) with forces larger than a critical value (30 mN here) are deemed as the same jamming event. For each jamming event, the duration of jammed state is the interval between the start point and end point, i.e. $\Delta t_i = t_{i,end} - t_{i,start}$, and the strength is the corresponding area in the plot of force F vs time t, i.e. $S_i = \int_{t_{i,start}}^{t_{i,end}} F dt$. Fig. 4 shows the variation of the characteristics of mechanical jamming with gap size, where only the cases with significant force peaks are included. Both duration and strength decrease sharply as the gap size is increased. Thus, the gap size is a dominant factor controlling mechanical jamming. Compared to powder A, the jamming duration and strength of powder B is larger, indicating that angular particles are more prone to mechanical jamming. Mechanical jamming of powder C is the weakest, suggesting that too strong cohesion may inhibit the occurrence of mechanical jamming. The complementary cumulative distribution function (CCDF) of both the duration and strength exhibits a power-law tail with an exponent larger than 2, as shown in the insets of Fig. 4.

Mechanical jamming could also be related to the quality of spread layer. Obvious evidence is the formation of empty patches, i.e. local regions on the baseplate which are not covered by particles, as shown in

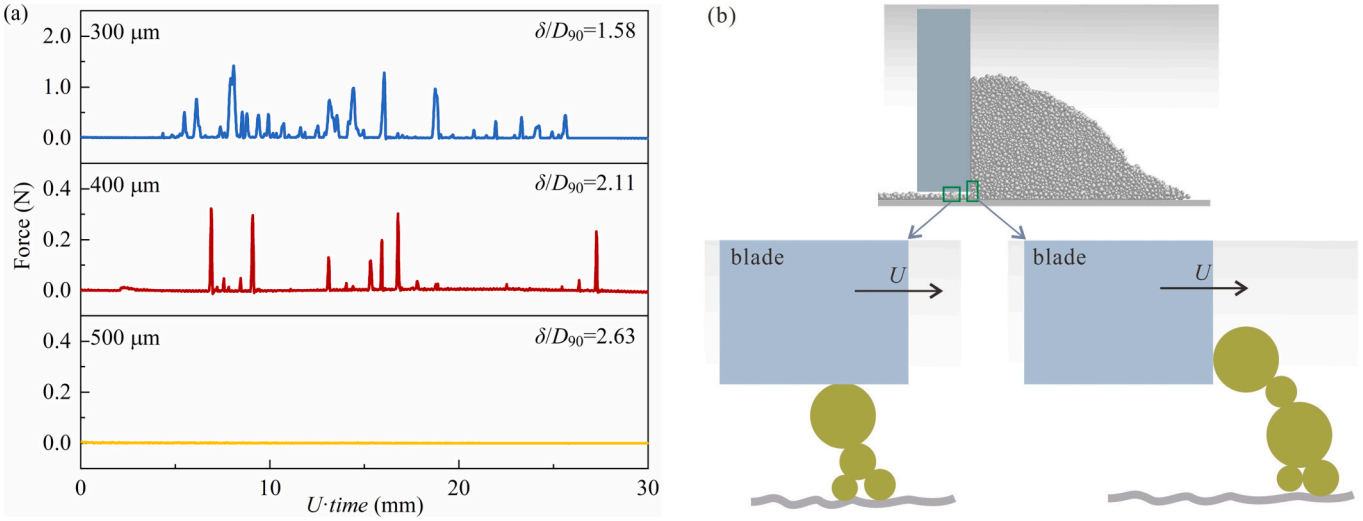

Fig. 3. Trace of the force of baseplate indicating of mechanical jamming: (a) variation of force on the baseplate with time under three gap sizes for powder B (D_{90} = 190 μm), where the time is scaled to the spread length by using blade speed U = 0.01 m/s; (b) schematics of two kinds of jammed state.

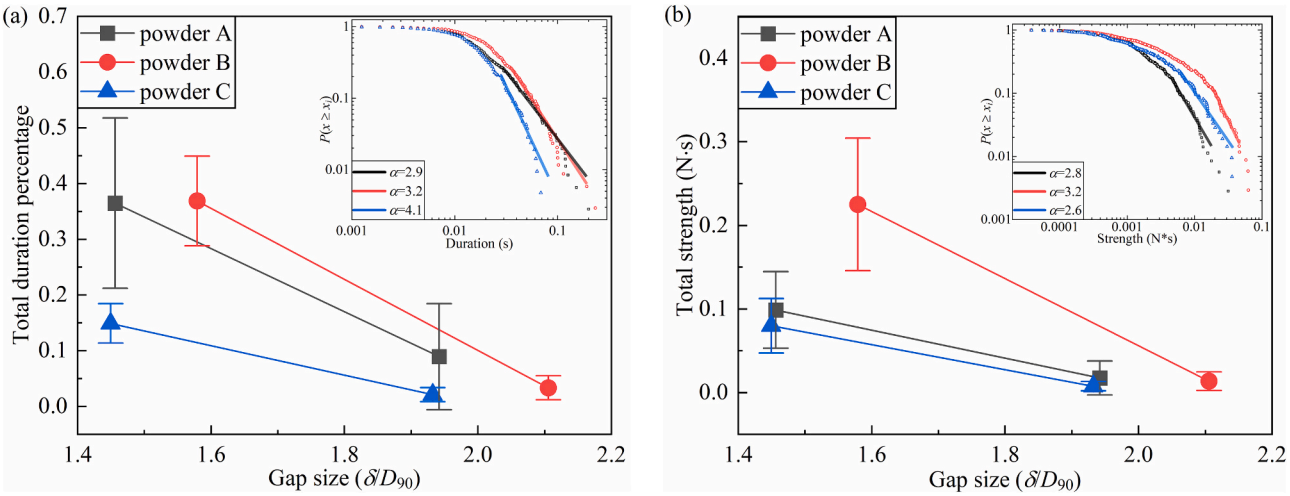

Fig. 4. Variation of the characteristics of mechanical jamming with gap size, (a): total duration percentage, i.e. total duration of jamming normalised by total spreading time of an individual experiment test; (b): total strength, i.e. summation of the strength of all jamming events in an individual experiment test; error-bar in (a) and (b) is the standard deviation for 11 experiment tests; sub-graphs in (a) and (b) are the complementary cumulative distribution function (CCDF) of jamming duration or strength for all jamming events observed in all 11 experiment tests, the tail of which are fitted by a power-law $x^{-\alpha}$ with p-value larger than 0.1.

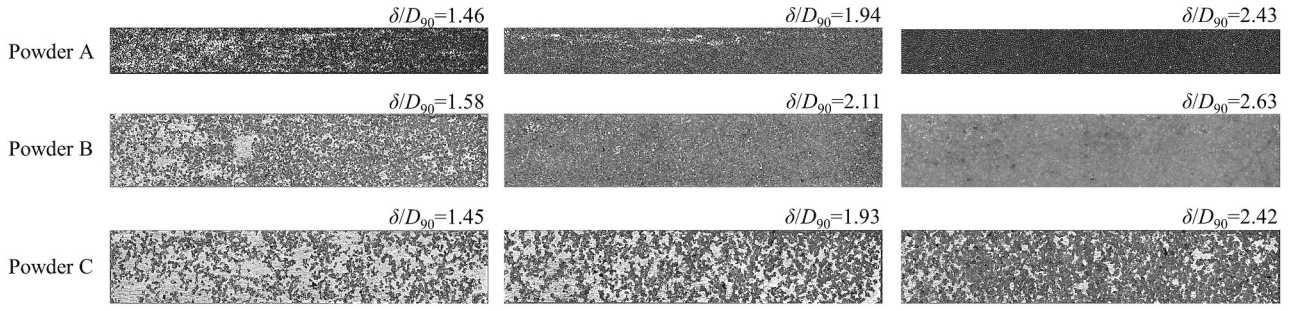

Fig. 5. Snapshots of particle layer after spreading for three kinds of powder, where the regions not covered by particles are called empty patches.

Fig. 5. Mechanical jamming has two adverse effects on the formation of spread layer: 1) the particle flow is transiently halted, resulting in not enough particles flowing out the gap during the survival period of jamming; 2) large strain energy is stored during the survival period of jamming, and this energy would release suddenly and kick away the jammed particles from the gap once the jamming state is broken by the moving blade, resulting in significantly non-uniform distribution of particles within the spread layer. With the increase of gap size, both the number and size of empty patches are reduced. As the gap size is increased to $\delta/D_{90} = 2.43$ for powder A and to $\delta/D_{90} = 2.63$ for powder B, the baseplate is almost fully covered by the particles. However, for powder C, there are still several empty patches even when the gap size increases to $\delta/D_{90} = 2.42$.

As shown in Fig. 6(a), total area percentage of empty patches

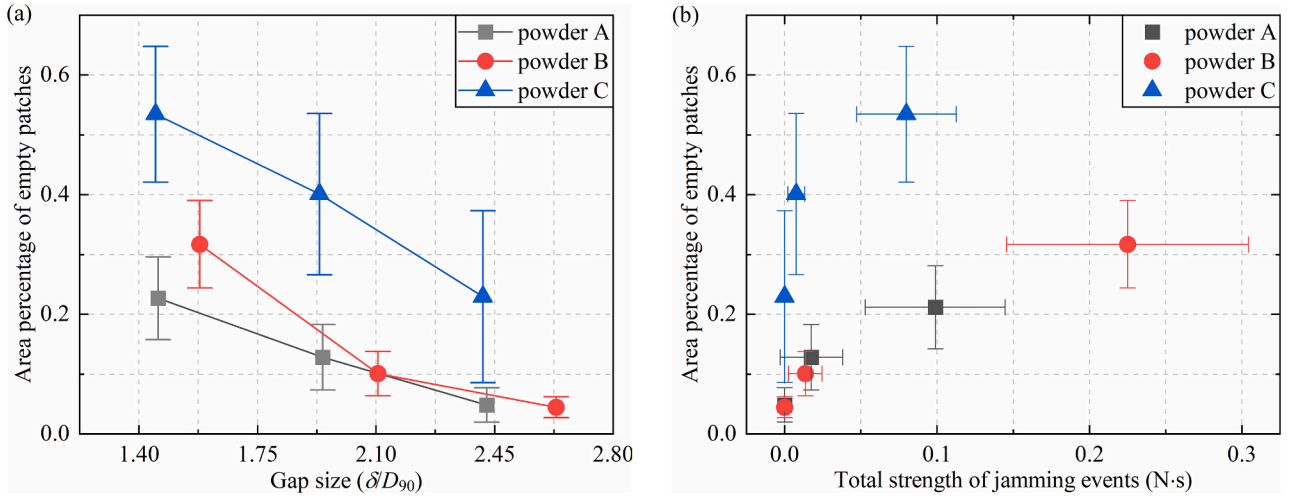

Fig. 6. Variation of the area percentage of empty patches with (a) gap size and (b) total jamming strength, where error-bar is the standard deviation.

decreases with the gap size. Compared to powder B, the area percentage of empty patches is much larger for powder C, indicating that the powder with strong cohesion is more prone to empty patches. For example, for powder C, the area percentage of empty patches is about 22% even when the gap size is $2.42D_{90}$, which is similar to that of powder A at $\delta/D_{90} = 1.46$. As shown in Fig. 6(b), for powder A and powder B, the area percentage of empty patches increases with the strength of mechanical jamming, validating that empty patches can be caused by mechanical jamming. However, for powder C, the empty patches are more prone than that of powder A and powder B at the same strength of mechanical jamming. Therefore, not all empty patches are due to mechanical jamming, and there should be another kind of jamming responsible for the formation of empty patches. Here, considering the fact that powder C has similar particle shape as powder B but much more cohesive due to binder coated on the particle surface, cohesion-induced jamming is assumed, in which no large force of the baseplate could be observed during spreading, but there are still a number of empty patches after spreading. For powder C at $\delta/D_{90} = 2.42$, the empty patches are mainly caused by strong cohesion between particles instead of mechanical jamming.

Based on above results, a jamming regime map is deduced for the blade spreading system of particles, as shown in Fig. 7. There is a transition between mechanical jamming and cohesion-induced jamming, depending on the gap size, interlocking and cohesion between particles, as well as the roughness of the baseplate. For purely mechanical jamming, it is mainly observed for cohesionless particles or particles with weak cohesion, and angular particles are more prone to mechanical jamming. For particles with strong cohesion, pure cohesion-induced jamming could be observed at large gap size, where the contact structure of jamming is fragile without strong contact force between clusters or agglomerates and wall, while both mechanical and cohesion-induced jamming may be formed at small gap size, where a strong interaction exists between the wall and particles. Additionally, there is a special case, i.e. particles slip on the baseplate due to very strongly cohesive interaction between particles during spreading or the effect of history compressing of bulk cohesive powder before spreading, in which almost no particles could be spread onto the baseplate, as shown in Fig. 8. For most kinds of particles, jamming could be avoided when the gap size is large enough, where the particles are continuously spread onto the baseplate, and the baseplate is fully covered by particles without any empty patches after spreading. For purely mechanical jamming, the critical gap size of un-jammed flow is $2–2.5D_{90}$, which is smaller than the ones in hopper flow [9]. This is due to the fact that only one wall (baseplate) is stationary in blade spreading system, while all walls are stationary in hopper flow. For particles with strong cohesion, larger critical gap size is demanded for continuous flow, depending on particle properties.

4. Conclusions

In this work, the transient jamming by blade spreading is explored by experiments, where the force on the baseplate and the empty patches within the spread layer are analysed. Mechanical jamming is transient and in a dynamic state, i.e. repetitively forming and collapsing under the combined effects of narrow gap and blade shearing action. This is much different to the static jamming in hopper flow. Mechanical jamming in blade spreading system is mainly controlled by the gap size. Angular particles are more prone to mechanical jamming, while too strong cohesion may inhibit its occurrence. Besides mechanical jamming, cohesion-induced jamming is also critical for the formation of empty patches. A jamming regime map is deduced for the blade spreading system of particles, including mechanical jamming, transition zone, cohesion-induced jamming, and slug (full slip). For most kinds of particles, jamming could be avoided when the gap size is large enough. The critical gap size is $2–2.5D_{90}$ for mechanical jamming, while larger critical gap size is demanded for particles with strong cohesion.

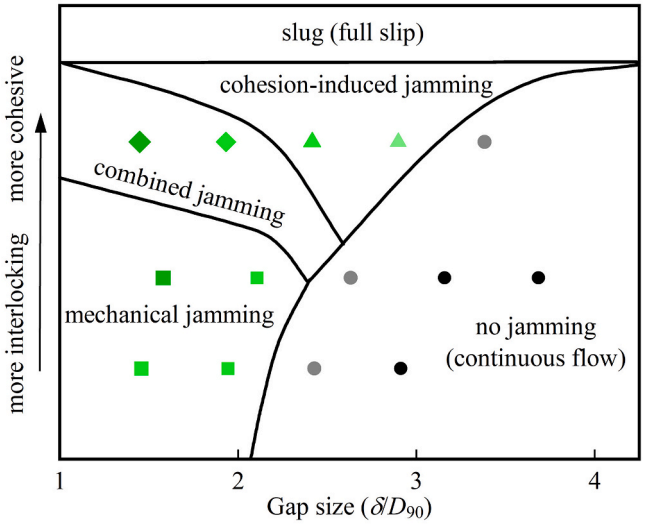

Fig. 7. Regime map of transient jamming in blade spreading system of particles: for powder A ($D_{90} = 103$ μm, the third row of symbols), the gap size is 150, 200, 250, and 300 μm; for powder B ($D_{90} = 190$ μm, the second row of symbols) and powder C ($D_{90} = 207$ μm, the first row of symbols), the gap size is 300, 400, 500, 600, and 700 μm.

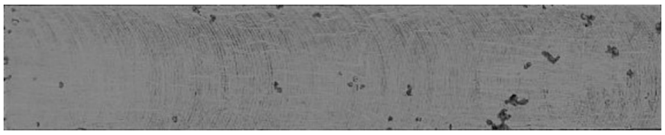

Fig. 8. Special regime with almost no particles being spread onto the baseplate, in which the particle heap slides on the baseplate as a slug in the blade spreading system: powder C at the gap size of 300 μm, and the powder heap is manually compressed before spreading.

CRediT authorship contribution statement

Wenguang Nan: Conceptualization, Formal analysis, Investigation, Writing – original draft, Writing – review & editing. **Lanzhou Ge:** Methodology, Formal analysis, Investigation. **Wenbin Xuan:** Methodology, Investigation. **Yiqing Gu:** Methodology.

Declaration of Competing Interest

The authors declare that they have no known competing financial interests or personal relationships that could have appeared to influence the work reported in this paper.

Data availability

Data will be made available on request.

Acknowledgements

The authors are grateful to the National Natural Science Foundation of China (Grant No. 51806099, U2241248). The first author is also grateful to the National Key Research and Development Program of China (Grant No. 2022YFB4602202). The corresponding author is also thankful to Professor Mojtaba Ghadiri, University of Leeds, UK, for his inspiration and valuable comments on this work. The authors are also thankful to Mr. Tianfu Fu, for his support and help on the set-up of the experiment.

Appendix

Variation of force on the baseplate with time for powder A and powder C is shown in Fig. A1, which is in a similar trend as powder B shown in **Fig. 3** (a).

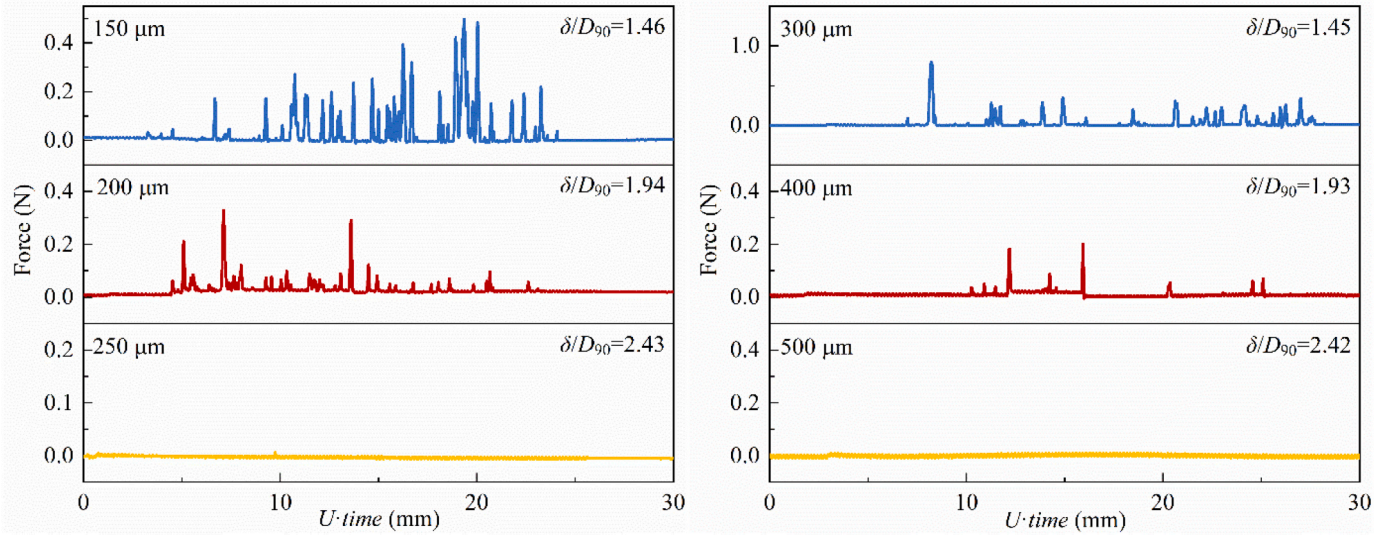

Fig. A1. Variation of force on the baseplate with time: powder A (left) and powder C (right), where the time is scale to spread length by blade speed $U = 0.01$ m/s.

References

[1] S. Haeri, Y. Wang, O. Ghita, J. Sun, Discrete element simulation and experimental study of powder spreading process in additive manufacturing, Powder Technol. 306 (2016) 45–54.

[2] P. Jop, Y. Forterre, O. Pouliquen, A constitutive law for dense granular flows, Nature 441 (2006) 727–730.

[3] M. Bouzid, M. Trulsson, P. Claudin, E. Clement, B. Andreotti, Nonlocal rheology of granular flows across yield conditions, Phys. Rev. Lett. 111 (2013), 238301.

[4] T.T. Vo, S. Nezamabadi, P. Mutabaruka, J.Y. Delenne, F. Radjai, Additive rheology of complex granular flows, Nat. Commun. 11 (2020) 1476.

[5] D.B. Nagy, P. Claudin, T. Borzsonyi, E. Somfai, Rheology of dense granular flows for elongated particles, Phys. Rev. E 96 (2017), 062903.

[6] S.A. Khairallah, A.A. Martin, J.R.I. Lee, G. Guss, N.P. Calta, J.A. Hammons, M. H. Nielsen, K. Chaput, E. Schwalbach, M.N. Shah, M.G. Chapman, T.M. Willey, A. M. Rubenchik, A.T. Anderson, Y.M. Wang, M.J. Matthews, W.E. King, Controlling interdependent meso-nanosecond dynamics and defect generation in metal 3D printing, Science 368 (2020) 660–665.

[7] W. Nan, M. Pasha, T. Bonakdar, A. Lopez, U. Zafar, S. Nadimi, M. Ghadiri, Jamming during particle spreading in additive manufacturing, Powder Technol. 338 (2018) 253–262.

[8] I. Zuriguel, D.R. Parisi, R.C. Hidalgo, C. Lozano, A. Janda, P.A. Gago, J.P. Peralta, L.M. Ferrer, L.A. Pugnaloni, E. Clement, D. Maza, I. Pagonabarraga, A. Garcimartin, Clogging transition of many-particle systems flowing through bottlenecks, Sci. Rep. 4 (2014) 7324.

[9] K. To, P.Y. Lai, H.K. Pak, Jamming of granular flow in a two-dimensional hopper, Phys. Rev. Lett. 86 (2001) 71–74.

[10] M.A. Aguirre, J.G. Grande, A. Calvo, L.A. Pugnaloni, J.C. Geminard, Pressure independence of granular flow through an aperture, Phys. Rev. Lett. 104 (2010), 238002.

[11] M.J. Cordero, L.A. Pugnaloni, Dynamic transition in conveyor belt driven granular flow, Powder Technol. 272 (2015) 290–294.

[12] A. Guariguata, M.A. Pascall, M.W. Gilmer, A.K. Sum, E.D. Sloan, C.A. Koh, D. T. Wu, Jamming of particles in a two-dimensional fluid-driven flow, Phys. Rev. E 86 (2012), 061311.

[13] P.G. Lafond, M.W. Gilmer, C.A. Koh, E.D. Sloan, D.T. Wu, A.K. Sum, Orifice jamming of fluid-driven granular flow, physical review, E, Statistical, nonlinear, and soft matter physics 87 (2013), 042204.

[14] D. Bi, J. Zhang, B. Chakraborty, R.P. Behringer, Jamming by shear, Nature 480 (2011) 355–358.

[15] E.J. Banigan, M.K. Illich, D.J. Stace-Naughton, D.A. Egolf, The chaotic dynamics of jamming, Nat. Phys. 9 (2013) 288–292.

[16] R.P. Behringer, Jamming in granular materials, C. R. Phys. 16 (2015) 10–25.

[17] W.G. Nan, M. Pasha, M. Ghadiri, Effect of gas-particle interaction on roller spreading process in additive manufacturing, Powder Technol. 372 (2020) 466–476.

[18] S. Khajepor, O. Ejtehadi, S. Haeri, The effects of interstitial inert gas on the spreading of Inconel 718 in powder bed fusion, Addit. Manuf. 75 (2023).

[19] C. Heussinger, J.-L. Barrat, Jamming transition as probed by quasistatic shear flow, Phys. Rev. Lett. 102 (2009).